Invest New Drugs (2011) 29:1347–1359
DOI 10.1007/s10637-010-9497-0

PRECLINICAL STUDIES

Protoapigenone, a natural derivative of apigenin, induces mitogen-activated protein kinase-dependent apoptosis in human breast cancer cells associated with induction of oxidative stress and inhibition of glutathione S-transferase π

Wen-Ying Chen · Yu-An Hsieh · Ching-I Tsai · Ya-Fei Kang · Fang-Rong Chang · Yang-Chang Wu · Chin-Chung Wu

Received: 27 March 2010 / Accepted: 13 July 2010 / Published online: 5 August 2010

Summary Protoapigenone, a natural derivative of the flavonoid apigenin, has been shown to exhibit potent antitumor activity in vitro and in vivo; the precise mechanism of action, however, is not fully elucidated. In this study, we investigated and compared the mechanisms by which protoapigenone and apigenin caused cell death in the human breast cancer MDA-MB-231 cells. Flow cytometry analysis revealed that protoapigenone induced apoptosis with 10-fold greater potency than apigenin. Cancer cells treated with protoapigenone resulted in persistent activation of mitogen-activated protein kinase (MAPK) ERK, JNK, and p38, hyperphosphorylation of Bcl-2 and Bcl-xL, and loss of mitochondrial membrane potential (MMP). The MAPK inhibitors effectively prevented the loss of MMP and apoptosis induced by protoapigenone. Treatment of cells with protoapigenone led to increased levels of reactive oxygen species (ROS) and decreased levels of intracellular glutathione. The thiol-antioxidant N-acetylcysteine abolished protoapigenone-induced MAPK activation, mitochondrial dysfunction, and apoptosis. These results suggest that the induction of oxidative stress preceding the activation of MAPK is required to initiate the mitochondria-mediated apoptosis induced by protoapigenone. Additionally, protoapigenone-induced JNK activation was linked to thiol modification of glutathione S-transferase π (GSTpi), which impeded GSTpi inhibition of JNK. In contrast to protoapigenone, apigenin-induced apoptosis was neither dependent on ROS nor on MAPK. Structure-activity relationship studies suggested that the thiol reacting effect of protoapigenone might be associated with an α, β-unsaturated ketone moiety in the structure of ring B.

Keywords Protoapigenone · Apigenin · Oxidative stress · Mitogen-activated protein kinases · Glutathione S-transferase π · Breast cancer

Abbreviations

CCCP	carbonyl-cyanide-m-chloro-phenyl-hydrazine
CDNB	1-chloro-2, 4-dinitrobenzene
GSTpi	glutathione S-transferase π
H2DCFDA	2′, 7′-dichlorodihydrofluorescein diacetate
MAPK	mitogen-activated protein kinase
MMP	mitochondrial membrane potential

W.-Y. Chen · Y.-F. Kang
School of Medicine and Health Sciences, Fooyin University, Kaohsiung 83101, Taiwan

Y.-A. Hsieh · C.-I. Tsai · F.-R. Chang · Y.-C. Wu (✉) · C.-C. Wu (✉)
Graduate Institute of Natural Products, Kaohsiung Medical University, 100 Shih-Chuan 1st Rd, Kaohsiung City 80708, Taiwan
e-mail: yachwu@kmu.edu.tw
e-mail: ccwu@kmu.edu.tw

Y.-C. Wu
College of Chinese Medicine, China Medical University, Taichung City, Taiwan

MTT	3-(4,5-dimethyl-thiazol-2-yl)-2,5-diphenyl tetrazolium bromide
NAC	N-acetylcysteine
PBS	phosphate-buffered saline
PI	propidium iodide
ROS	reactive oxygen species
zVAD-fmk	Z-Val-Ala-Asp (OMe)-fluoromethyl ketone

Introduction

Breast cancer is the second-most common and leading cause of cancer death among women [1]. Although chemotherapy is routinely used in the treatment of metastatic breast cancer; a large proportion of the patients does not benefit from the treatment and may suffer from severe adverse effects [2, 3]. Therefore, there is an urgent need to develop mechanism-based strategies and to discover new potential anti-cancer drugs for the treatment of metastatic breast cancer.

Plant-derived flavonoids have recently received a great deal of attention because of their antioxidant, antiviral, antiplatelet, anti-mutagenic, anti-inflammatory, and antitumor activities [4–6]. Flavonoids such as quercetin, luteolin and apigenin were expected to be not only a promising cancer-preventive agent contained in foods but also a candidate of chemotherapeutic agents [7, 8]. In our previous study, seven flavonoids were isolated from *Thelypteris torresiana* using bioactivity-guided fractionation methods [9]. Among them, a novel flavone protoapigenone exhibited significant anti-tumor activities toward HepG2, Hep3B, MCF-7, A549, and MDA-MB-231 with IC_{50} values ranging from 0.23 to 3.88 μM. Follow-up studies showed that protoapigenone decreased the viability of cancer cells through induction of cell cycle arrest and apoptosis [10, 11]. In a nude mouse xenograft model, protoapigenone also exhibited significant antitumor activity against human ovarian cancer cells and prostate cancer cells [10, 11]. In addition, the proapoptotic effect of protoapigenone was due to, at least in part, its ability to activate JNK and p38 in cancer cells [11]; however, the precise mechanism accounting for this effect remains unclear.

In this study, we investigated the anticancer effect and the mechanism of action of protoapigenone in MDA-MB-231 cells, which are highly metastatic human breast cancer cells. Moreover, apigenin, one of the most common flavonoids with a structure similar to protoapigenone, was examined in parallel with protoapigenone to determine the possible structure-activity relationships. Our results show for the first time that protoapigenone, but not apigenin, induced apoptosis through oxidative stress-mediated MAPK activation, and this activity may be associated with an α, β-unsaturated ketone moiety in the ring B of protoapigenone.

Materials and methods

Drugs and chemicals

Protoapigenone (Fig. 1a) was isolated from *Thelypteris torresiana* as described previously [9] with purities exceeding 98% as determined by HPLC. Protoapigenone was dissolved in DMSO, and the final concentration of DMSO in culture medium was 0.2%. Anti-JNK polyclonal antibody was purchased from Upstate. Anti-phopho-p38 and anti-GSTpi (3F2) antibodies were purchased from Cell Signaling Technology; all other antibodies were from Santa Cruz Biotechnology Inc. 2′,7′-Dichlorodihydrofluorescein diacetate (H_2DCFDA), monochloromobimane, and $DiOC_{6(3)}$ were obtained from Molecular Probes (Eugene, OR). Z-Val-Ala-Asp (OMe)-fluoromethyl ketone (zVAD-fmk) was obtained from Calbiochem (Biosciences, Inc). Apigenin, λ-phosphatase, U0126, SP600125, SB202190, N-acetylcysteine (NAC), 3-(4,5-dimethyl-thiazol-2-yl)-2,5-diphenyl tetrazolium bromide (MTT), propidium iodide (PI) and all other chemicals were obtained from Sigma Chemical Co.

Cell culture

MDA-MB-231 human breast cancer cells were obtained from American Tissue Culture Collection. Cells were incubated at 37°C in a humidified atmosphere containing 5% CO_2 in RPMI 1640 medium, supplemented with 10% fetal bovine serum, penicillin (100 IU/ml) and streptomycin (100 μg/ml). The cells were harvested by trypsinization and plated 24 h before treatment with the test drugs.

Evaluation of cell viability

1×10^4 cells were plated into each well of a 96-well plate and treated with the various concentrations of drugs for different indicated times. At the end of each time point, 100 μl of MTT solution (0.5 mg/ml) was added to each well. Cells were then incubated at 37°C for 1 h. The MTT crystals in each well were solubilized in 100 μl of DMSO. Absorbance was read at 550 nm.

Measurement of DNA fragmentation

2×10^5 cells were seeded onto each well of a 6 well plate and treated with the various concentrations of drugs for the indicated times. At the end of each time point, cells were trypsinized, washed with ice-cold phosphate-buffered saline (PBS), and then fixed overnight in 70% ethanol at 4°C.

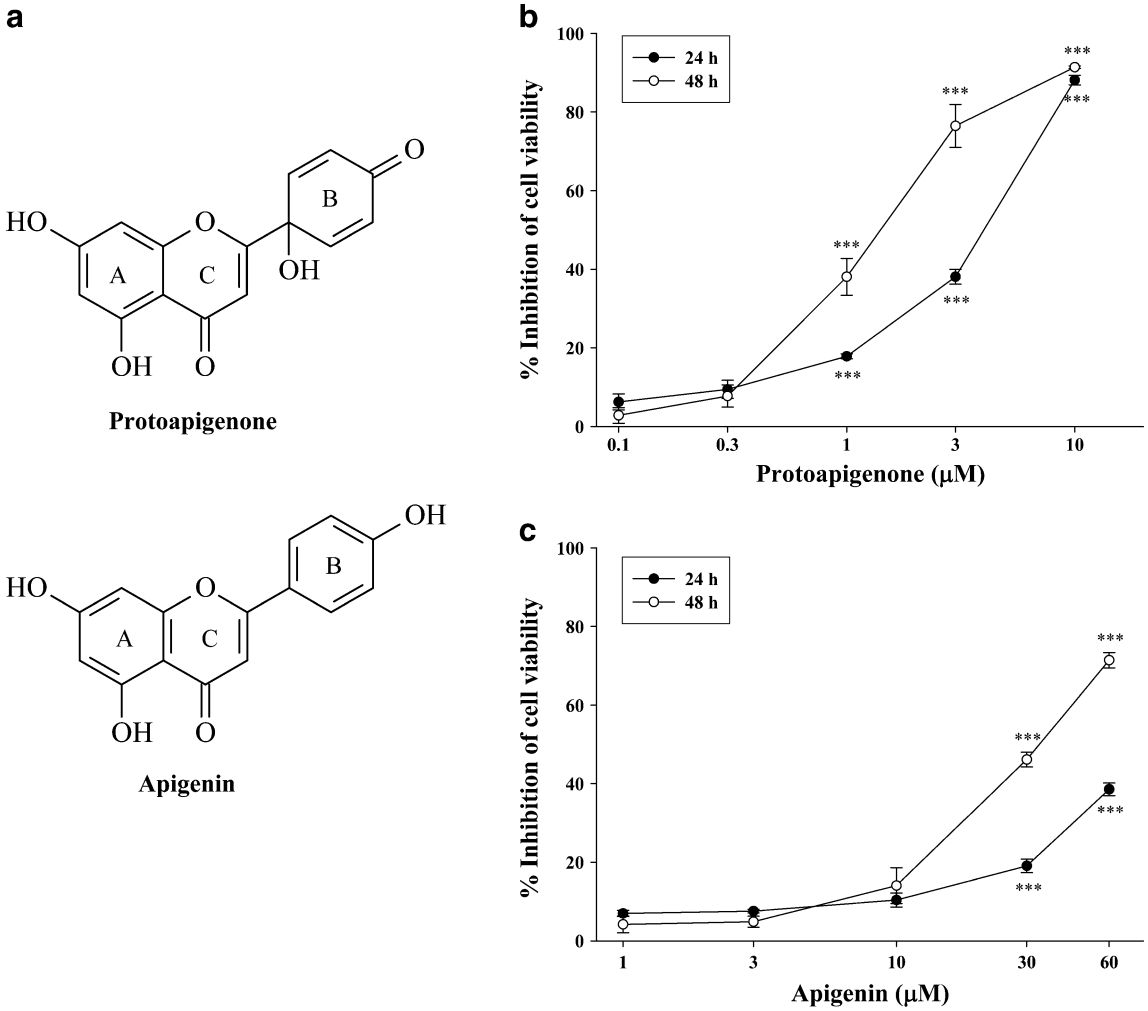

Fig. 1 Effects of protoapigenone and apigenin on cell viability of MDA-MB-231 cells. (**a**) Chemical structures of protoapigenone and apigenin. MDA-MB-231 cells were treated with the indicated concentrations of protoapigenone (**b**) or apigenin (**c**) for 24 and 48 h, respectively, and cell viability was determined by the MTT assay, Results are presented as means±S.E.M. (n=3)

After fixation, cells were washed and incubated in PBS containing 25 μg/ml RNase and 0.5% Trition-X100 for 1 h at 37°C. Finally, cells were stained with 50 μg/ml propidium iodide (PI) for 15 min at 4°C in the dark. The DNA content of cells was quantified by FACScan flow cytometry (Beckman Coulter, EPICS XL-MCL). The percentage of cells with hypodiploid DNA content ($subG_1$) represented fraction undergoing apoptotic DNA fragmentation.

Annexin V/PI staining

2×10^5 cells were seeded onto each well of a 6-well plate and treated with DMSO or protoapigenone for different indicated times. Harvested cells were washed with PBS and stained with annexin V and PI for 15 min at room temperature in the dark according to the manufacturer's protocol (BD Pharmingen). Apoptotic cells were quantified by FACScan flow cytometry (Beckman Coulter, EPICS XL-MCL). Stained cell populations were defined as: lower left quadrant, living cells (annexin V^-/PI^-); lower right quadrant, early apoptotic cells (annexin V^+/PI^-); upper right quadrant, late apoptotic cells (annexin V^+/PI^+); upper left quadrant, primary necrotic cells (annexin V^-/PI^+).

Assessment of mitochondrial membrane potential (MMP)

The change of MMP was determined as described previously with some modifications [12]. 3×10^5 cells were seeded onto each well of a 6 well plate and treated with the test drugs for the indicated times. At the last 30 min of the incubation period, cells were loaded with 40 nM $DiOC_{6(3)}$ in the dark. The cells were then harvested and resuspended in ice-cold PBS. The fluorescence intensities of cells were measured immediately by flow cytometry, at respective wavelengths for excitation and emission of 484 and 500 nm.

Western blot assay

Western blot analysis was performed as previously described [13]. Cell lysates were prepared and proteins were separated by SDS-PAGE and transferred to a nitrocellulose membrane, followed by visualization using the enhanced chemiluminescence (ECL) reagent (Amersham Pharmacia Biotech). For analysis of disulfide-bonded protein by non-reducing SDS-PAGE, drug-treated cells were washed with PBS at the indicated times and then incubated with iodoacetamide (40 mM) for 5 min to prevent thiol-disulfide exchange and post-lysis oxidation of free cysteines [14]. Moreover, samples were diluted in SDS-sample buffer without reducing agents before loading onto SDS-polyacrylamide gels.

Detection of reactive oxygen species

The intracellular accumulation of ROS, including H_2O_2 and other peroxides, was monitored using the fluorescent probe H_2DCFDA [15, 16]. At the end of the treatments, cells were loaded with 20 μM H_2DCFDA and incubated at 37°C for 30 min in the dark. Cells were then collected and resuspended in PBS. The fluorescence was measured immediately by flow cytometry.

Determination of intracellular glutathione levels

The content of intracellular glutathione was determined using monochlorobimane [17]. Briefly, after treatments, cells in 96-well plates were loaded with 100 μM monochlorobimane for 30 min in the dark. Then, plates were read on a micro-plate reading fluorometer using excitation and emission wavelengths of 390 and 460 nm, respectively.

Determination of JNK-GSTpi association by immunoprecipitation (IP)

Anti-JNK rabbit antibody was conjugated to magnetic beads (Dynabeads Protein A, Invitrogen) according to the manufacturer's protocol. Cells were harvested and lysed in lysis buffer (50 mM Tris–HCl, 150 mM NaCl, 1 mM EDTA, 1 mM EGTA, 1% Triton-X100, 20 μg/ml leupeptin, 2 mM sodium orthovanadate, 1 mM phenylmethylsulfonyl-fluoride, 5 mM sodium fluoride, and 5,000 U/ml aprotinin). Cell lysates (300 μg protein) were incubated with anti-JNK antibody- conjugated Dynabeads in IP buffer (50 mM Tris-HCl at pH 8.0, 150 mM NaCl, 1% NP-40, and protease inhibitors) for 1 h at 4°C. Beads were captured using a magnetic particle concentrator (Invitrogen). After three washes in 0.5 ml of IP buffer, beads were resuspended and boiled in 40 μl of Laemmli reducing sample buffer. The eluates were subjected to SDS-PAGE. Mouse monoclonal anti-GSTpi (1:1000), and mouse anti-JNK (1:1000) antibody were used as primary antibodies and detected by ECL reagent.

Assay of GSTpi activity

Cell lysates were prepared and aliquots of the supernatant were used to measure the GSTpi activity according to the method of Habig et al. [18]. The reaction mixture was carried out in 0.1 M potassium phosphate buffer with 1 mM EDTA (pH 6.5), containing 1 mM glutathione, and 0.5 mM 1-chloro-2, 4-dinitrobenzene (CDNB). Enzyme activity was measured spectrophotometrically at 340 nm for 5 min. The rate of spontaneous conjugation of glutathione to CDNB was subtracted from the rates of GSTpi-catalyzed reaction. GSTpi activity was defined as the amount of enzyme that was able to catalyze the conjugation of 1 nmol of CDNB with glutathione per minute at 25°C, and it was referred to as the protein content of each sample. The results of the inhibition assays are presented as percentage of control values.

Statistics

Data are presented as means±S.E.M. and comparisons were made using Student's *t* test. A probability of 0.05 or less was considered statistically significant.

Results

Protoapigenone causes cytotoxicity in MDA-MB-231 cells

To examine the cytotoxicity of protoapigenone, MDA-MB-231 cells were treated with increasing concentrations of protoapigenone for up to 48 h and cell viability was determined by the MTT assay. Figure 1b showed that protoapigenone reduced cell viability of MDA-MB-231 cells in a concentration- and time-dependent manner. The IC_{50} value of protoapigenone was 4.7 μM and 1.6 μM at 24 and 48 h after treatment, respectively. In contrast, much higher concentrations of apigenin were required to inhibit the cell viability of MDA-MB-231 cells (IC_{50}=34.6 μM at 48 h after treatment, Fig. 1c).

Caspases are involved in protoapigenone-induced apoptosis

To explore whether cytotoxicity of protoapigenone was associated with the induction of apoptosis, MDA-MB-231 cells were treated with 3 or 10 μM protoapigenone for up to 48 h and the ploidy state of cells was analyzed by flow cytometry after propidium iodide (PI) staining nuclei. As shown in Fig. 2a, protoapigenone induced a concentration- and time-dependent increase in the proportion of subG1 population, suggesting that the cells underwent DNA fragmentation which is a hallmark of apoptosis. At 48 h, the

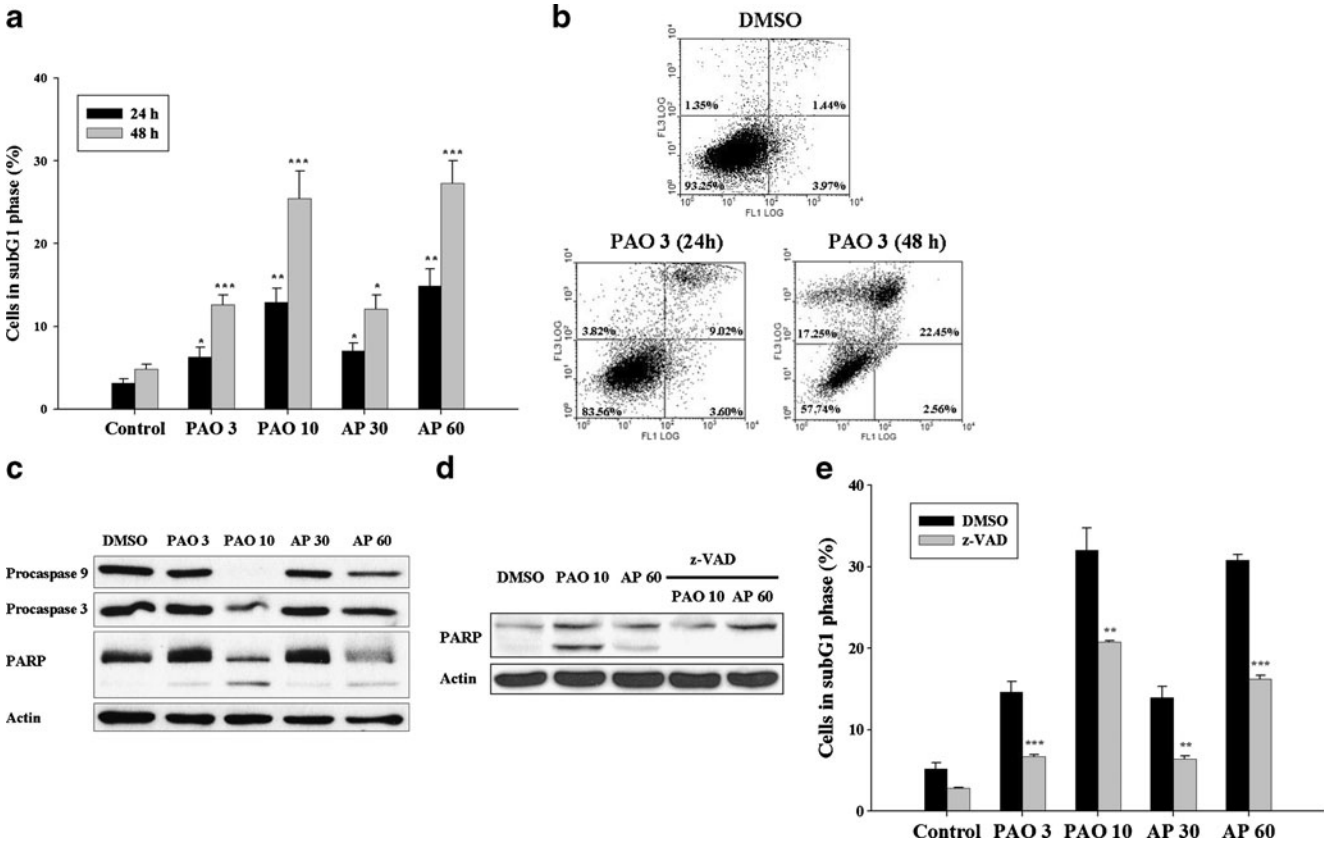

Fig. 2 Protoapigenone and apigenin induce caspase-dependent apoptosis in MDA-MB-231 cells. (**a**) Cells were treated with the indicated concentrations of protoapigenone or apigenin for 24 and 48 h, respectively. Apoptosis was determined by flow cytometry analysis of DNA fragmentation of PI-stained nuclei. (**b**) Cells were treated with protoapigenone (3 μM) for 24 and 48 h, respectively. After incubation, cells were stained with annexin V and PI and analyzed by flow cytometry. (**c**) Cells were treated with protoapigenone (3 and 10 μM) or apigenin (30 and 60 μM) for 24 h. Total cell lysates were prepared and aliquots containing 100 μg of protein were subjected to SDS-PAGE followed by Western blot analysis with the antibodies indicated. (**d** and **e**) Cells were pretreated with or without zVAD-fmk (100 μM) for 1 h and followed by the treatment of protoapigenone or apigenin for another 48 h. The cleavage of PARP (**d**) and the percentage of subG$_1$ cells (**e**) were determined by Western blot and flow cytometry, respectively. Results in (**a**) and (**e**) are presented as mean±S.E.M. (n=3). $^{**}P<0.01$, $^{***}P<0.001$ as compared with the respective control

subG1 population increased significantly from 4.8% in the control to 12.6% and 25.5% in cells treated with 3 and 10 μM protoapigenone, respectively. Apigenin also induced DNA fragmentation in MDA-MB-231 cells, but the potency was about 10-fold less than that of protoapigenone. In order to further confirm that protoapigenone induces apoptosis, MDA-MB-231 cells treated with the drug were double stained with annexin V-FITC and PI, and analyzed by flow cytometry. Annexin V and PI staining allows to discriminate between living cells (annexin V^-/PI^-), early apoptotic cells (annexin V^+/PI^-), late apoptotic cells (annexin V^+/PI^+), and primary necrotic cells (annexin V^-/PI^+). Figure 2b shows that treatment of MDA-MB-231 cells with protoapigenone (3 μM) for 24 h or 48 h induced apoptosis (annexin V-positive cells, right quadrants) in a time-dependent manner. At 48 h, the PI-positive only population also significantly increased in protoapigenone-treated cells, suggesting that prolonged exposure of the drug could induce necrotic death. We next examined the role of caspases in protoapigenone-induced apoptosis. The activation of caspases was determined by a decrease in pro-enzyme levels using Western blot analysis. Figure 2c showed that the protein levels of procaspase-9 and -3 were significantly decreased in MDA-MB-231 cells after exposure of protoapigenone (10 μM) or apigenin (60 μM) for 24 h. The activation of caspase-3 was further confirmed by detecting the degradation of PARP, which is a DNA repair enzyme and undergo cleavage by caspase-3 during apoptosis. When MDA-MB-231 cells were pretreated with the general caspase inhibitor zVAD-fmk, both protoapigenone- and apigenin-induced cleavage of PARP were prevented; however, apoptosis caused by these two flavones were only partially reversed (Fig. 2d and e).

Protoapigenone causes the mitochondrial dysfunction and Bcl-2 and Bcl-xL phosphorylation

To further confirm whether mitochondria-mediated pathway was involved in protoapigenone and/or apigenin-

induced apoptosis, the changes of MMP were measured by flow cytometry using $DiOC_{6(3)}$. The mitochondrial uncoupler CCCP was used as a positive control for the reduction of MMP. As shown in Fig. 3a, CCCP (10 μM) induced a significant decrease in MMP at 6 h and 12 h after treatment. In a similar manner, protoapigenone and apigenin also induced remarkable losses of MMP after 6 h and 12 h of treatment, indicating mitochondrial dysfunction occurred at the early stage of apoptosis.

Next, we examine whether mitochondrial dysfunction induced by protoapigenone and apigenin were associated with a change in the expression of Bcl-2 family proteins. As shown in Fig. 3b, neither protoapigenone nor apigenin significantly affected the protein levels of Bax, Bcl-2, and Bcl-xL. However, protoapigenone treatment caused a mobility shift of Bcl-2 and Bcl-xL on SDS-PAGE, and the change in mobility was prevented when the cell lysates were treated with λ phosphatase before electrophoresis (Fig. 3c). These results clearly demonstrated that protoapigenone was capable of induction of Bcl-2 and Bcl-xL hyperphosphorylation. In contrast, apigenin had no such effect on the Bcl-2 family proteins.

Protoapigenone-induced Bcl-2 and Bcl-xL phosphorylation are associated with the MAPK pathways

Numerous studies have suggested that MAPKs play an important role in cells growth and apoptosis [19, 20]. Besides, activation of the JNK signaling pathway leads to the phosphorylation of many proteins, including Bcl-2 and Bcl-xL [21, 22]. To examine whether protoapigenone and apigenin activated MAPKs in MDA-MB-231 cells, the changes in the activity of MAPKs, including ERK, JNK, and p38 were determined by immunoblotting with antibodies specifically recognizing the active phosphorylated forms. In both protoapigenone (10 μM)- and apigenin (60 μM)-treated MDA-MB-231 cells, activation of ERK was detectable within 1 h and peaked at 12 h after drug addition (Fig. 4a). Protoapigenone also induced remarkable and lasting activation of JNK and, to a less extent, activation of p38. In contrast,

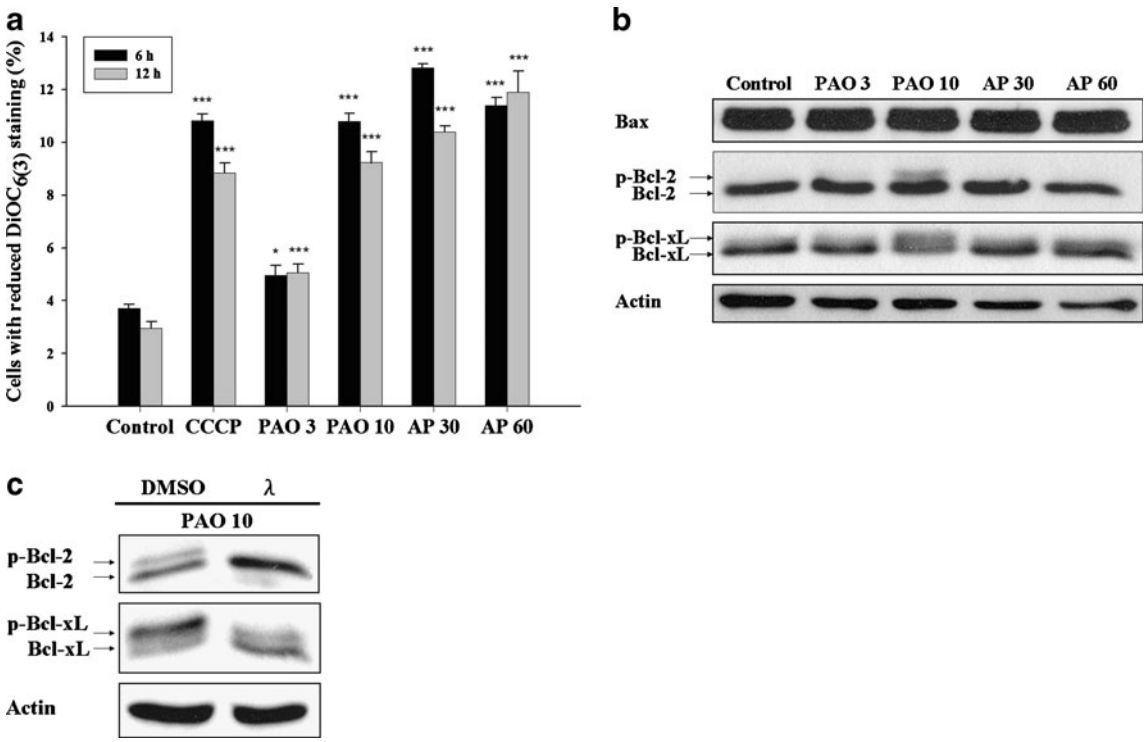

Fig. 3 Effects of protoapigenone and apigenin on mitochondrial membrane potential (MMP) and Bcl-2 family proteins. (**a**) MDA-MB-231 cells were treated with indicated concentrations of protoapigenone or apigenin for 6 or 12 h. Carbonyl-cyanide-m-chloro-phenyl-hydrazine (CCCP, 10 μM) was used as a positive control. The change in MMP was determined by flow cytometry using $DiOC_{6(3)}$ fluorescence dye (40 nM), which was added to media for the last 30 min of incubation. Results are presented as means±S.E.M. (n=3). *P<0.05, ***P<0.001 as compared with the respective control. (**b**) Cells were treated with indicated concentrations of protoapigenone or apigenin for 24 h. Total cell lysates were prepared and subjected to SDS-PAGE followed by Western blot analysis with the antibodies indicated. (**c**) After cells were treated with protoapigenone (10 μM) for 24 h, cell lysate was incubated with or without λ phosphatase (20,000 U/ml) for 30 min at 30°C. The phosphorylation states of Bcl-2 and Bcl-xL proteins were detected by Western blot analysis

apigenin induced significant p38 activation within 1 h, reached a peak at 6 h, and declined toward base line at 12 h after treatment. In order to examine whether the activation of MAPKs was required for protoapigenone- and apigenin-induced apoptosis, MDA-MB-231 cells were pretreated with the ERK inhibitor U0126, the JNK inhibitor SP600125, or the p38 inhibitor SB202190 before the addition of protoapigenone or apigenin. After a 48 h treatment of protoapigenone, U0126, SP600125, and SB202190 decreased the percentage of apoptotic cells ($SubG_1$) from 25.5% to 9.2%, 10.5%, and 11.6%, respectively (Fig. 4b). Moreover, protoapigenone-induced collapse of MMP and Bcl-2 phosphorylation were also prevented by the MAPK inhibitors (Fig. 4c and d). These results indicated that MAPKs performed crucial functions and might lie upstream of the Bcl-2 family in protoapigenone-induced apoptotic cascade. In contrast, these specific MAPK inhibitors failed to decrease apoptosis induced by apigenin (Fig. 4b), suggesting that MAPKs did not play a role in apigenin-induced apoptosis, despite these kinases were activated in apigenin-treated cells.

Protoapigenone induces change of redox status in MDA-MB-231 cells

Since oxidative stress is a mediator of apoptotic cell death and MAPKs are the major oxidative stress-sensitive signal transduction molecules [23, 24], we sought to determine whether protoapigenone could alter the redox status in

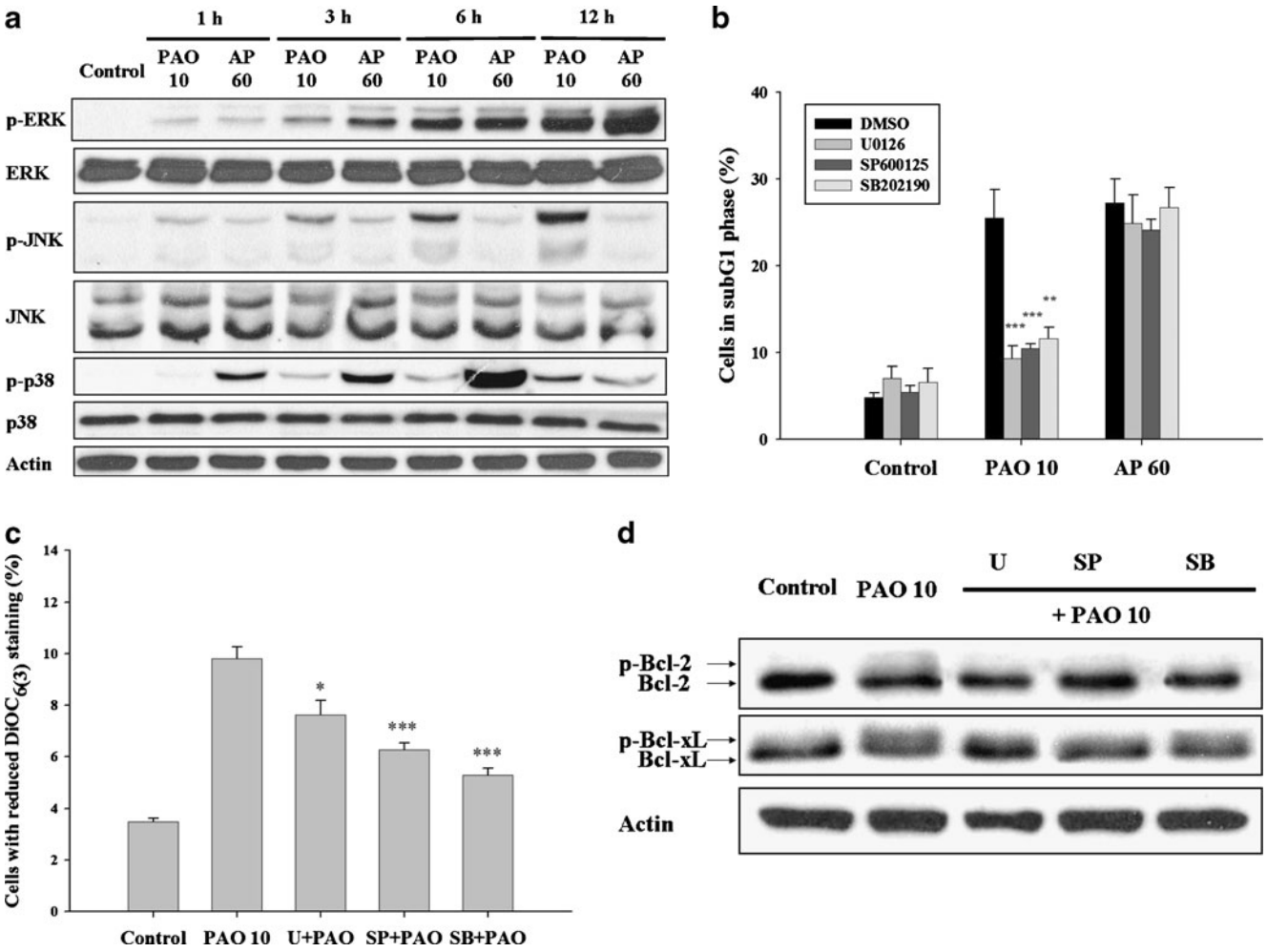

Fig. 4 Activation of MAPKs were involved in protoapigenone-, but not apigenin, induced apoptotic events. (**a**) Cells were treated with protoapigenone (10 μM) or apigenin (60 μM) and harvested at the indicated times. Total cell lysates were prepared and subjected to SDS-PAGE followed by Western blot analysis with the antibodies indicated. (**b**) Cells were pretreated with or without U0126 (U, 2 μM), SP600125 (SP, 15 μM), or SB202190 (SB, 15 μM) for 4 h, and followed by the treatment of protoapigenone (10 μM) or apigenin (60 μM) for another 48 h. Apoptosis was assessed by sub-G1 DNA contents. (**c**) Cells were pretreated with the MAPK inhibitors as mentioned above, and followed by the treatment of protoapigenone for another 6 h. After treatment, cells were stained with $DiOC_{6(3)}$ and the change in MMP were analyzed by flow cytometry. Results in (**b**) and (**c**) are presented as means±S.E.M. (n=3). *P<0.05, **P<0.01, ***P<0.001 as compared with the respective control. (**d**) After pretreatment of the MAPK inhibitors for 4 h, cells were challenged with protoapigenone (10 μM) and incubated for another 24 h. The protein levels of Bcl-2 and Bcl-xL were analyzed by Western blot

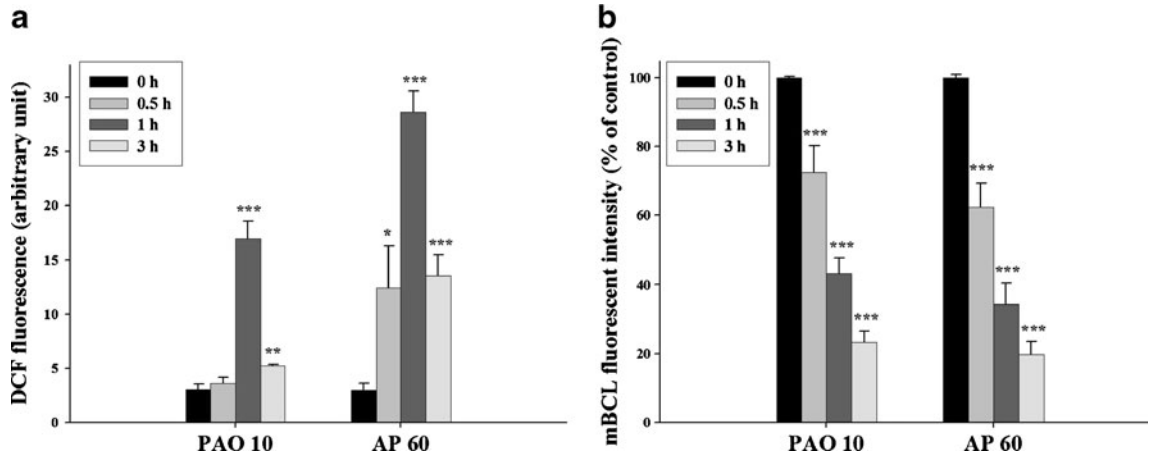

Fig. 5 Effects of protoapigenone and apigenin on redox state in MDA-MB-231 cells. (**a**) Cells were treated with protoapigenone (10 μM) or apigenin (60 μM) for indicated periods. After treatments, cells were loaded with H_2DCFDA (10 μM) to determine ROS generation and analyzed by flow cytometry. (**b**) After treatment of protoapigenone (10 μM) or apigenin (60 μM) for the indicated times, cells were loaded with monochlorobimane (100 μM) for determining intracellular glutathione contents. Results are presented as mean±S.E. M. of 3 independent experiments. *$P<0.05$, **$P<0.01$, ***$P<0.001$ as compared with the respective control

MDA-MB-231 cells. Figure 5a showed that protoapigenone (10 μM) induced a transient ROS burst at 1 h and declined at 3 h after treatment. Coincidently, total contents of intracellular glutathione decreased after protoapigenone treatment in a time-dependent manner (Fig. 5b). Similar to protoapigenone, apigenin (60 μM) also induced an increase in the intracellular ROS levels and a decrease in the intracellular glutathione contents (Fig. 5a and b). These results suggested that both protoapigenone and apigenin disturbed intracellular redox balance and elicited oxidative stress in MDA-MB-231 cells.

N-acetylcysteine prevents protoapigenone-induced responses in MDA-MB-231 cells

We next wanted to determine whether oxidative stress plays a role in protoapigenone and apigenin-induced apoptosis. Pretreatment of MDA-MB-231 cells with a thiol-antioxidant N-acetylcysteine (NAC, 2.5 mM) for 1 h prevented protoapigenone-induced ROS formation and glutathione depletion (Fig. 6 a and b). Furthermore, NAC suppressed protoapigenone-induced apoptosis, MMP collapse, caspase activation, PARP cleavage, and phosphorylation of Bcl-2 family proteins and MAPKs (Fig. 6 c, d, and e). In contrast, although NAC also prevented apigenin-induced oxidative stress (Fig. 6 a and b), it had no effects on apigenin-induced MAPK activation and apoptosis (Fig. 6c, e, and f). To confirm the generality of the results, we tested the effects of the flavonoids on another human breast cancer cell line MCF-7 and an oral squamous cell carcinoma cell line Ca9-22. Our results showed that both protoapigenone and apigenin induced apoptosis in these two cancer cell lines; however, only the proapoptotic effect of protoapigenone could be significantly prevented by NAC (Fig. 6g).

Protoapigenone induces dissociation of the JNK-GSTpi complex by thiol modification of GSTpi

Glutathione S-transferases (GSTs) have been shown to be endogenous inhibitors of MAPKs. It was reported that GSTpi binds to and inhibits JNK via protein-protein interaction. The inhibition of JNK activity by GSTpi can be reversed by oxidative stress, which causes oligomerization of GSTpi and dissociation of the GSTpi-JNK complex and consequently, leads to JNK activation [25, 26]. Therefore, we intended to examine whether protoapigenone-induced JNK activation was due to the disruption of GSTpi-JNK complex. MDA-MB-231 cells were treated with protoapigenone (10 μM) for up to 6 h, and then the cell lysates were immunoprecipitated with anti-JNK antibody and subjected to Western blot analysis. As shown in Fig. 7a, GSTpi co-precipitated with JNK was markedly reduced after 3 h treatment of protoapigenone, indicating that protoapigenone induced dissociation of JNK and GSTpi at very early timepoints during apoptosis.

We next determined whether protoapigenone disrupted GSTpi-JNK complex through thiol modification of GSTpi. Non-reducing SDS-PAGE revealed that when cells were treated with either protoapigenone (10 μM) or H_2O_2 (250 μM) for up to 6 h, the amounts of monomer form of GSTpi were decreased, while some higher molecular weight bands corresponding to disulfide-linked GSTpi were increased (Fig. 7b). To verify whether the GSTpi activity was affected by the thiol oxidation caused by protoapigenone, the GSTpi enzyme activity was evaluated both in intact cells and in a cell-free system. Figure 7c shows that when MDA-MB-231 cells were treated with protoapigenone (10 μM) for 6 h, the GSTpi enzyme activity was decreased to 66.0% of the control value. In the cell-free

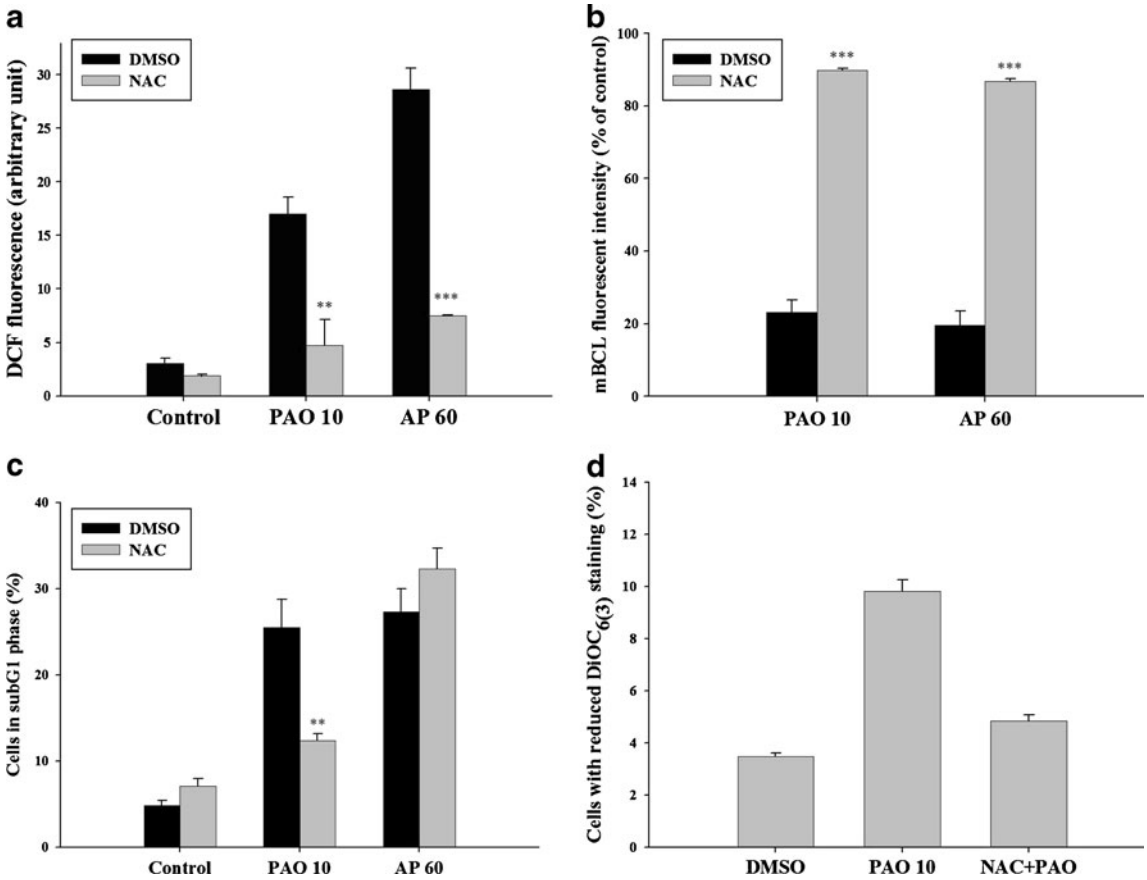

Fig. 6 Effects of N-acetylcysteine (NAC) on protoapigenone- and apigenin-induced responses in MDA-MB-231 cells. Cells were pretreated with or without NAC (2.5 mM) for 1 h, and followed by the treatment of protoapigenone (10 μM) or apigenin (60 μM) for another 1 h (**a**), 3 h (**b**), 6 h (**d**), 24 h (**e**, **f**), or 48 h (**c**). Flow cytometry was used to analyze ROS generation (**a**), intracellular glutathione contents (**b**), the proportion of cells in subG$_1$ phase (**c**), and the loss of MMP (**d**). (**g**) MCF-7 and Ca9-22 cells were treated with protoapigenone (10 μM) or apigenin (60 μM) for 48 h in the absence or presence of NAC (2.5 mM). After incubation, the proportion of cells in subG$_1$ phase was analyzed by flow cytometry. Results are presented as mean±S.E.M. of 3 independent experiments. $^{**}P<0.01$, $^{***}P<0.001$ as compared with the respective control. (**e** and **f**) Total cell lysates were prepared and subjected to SDS-PAGE followed by Western blot analysis with the antibodies indicated

system, MDA-MB-231 cell lysates were incubated with protoapigenone for 10 min at 25°C, the enzyme activity was also reduced and the IC_{50} value for protoapigenone was 26.3±4.8 μM. Ethacrynic acid, a known inhibitor of GSTpi, inhibited GSTpi activity in cell lysates with an IC_{50} value of 6.0±2.1 μM. However, a higher concentration of ethacrynic acid (200 μM) was required to effectively inhibit GSTpi in intact cells (Fig. 7c).

Discussion

In this study, we demonstrated that both apigenin and its derivative protoapigenone induced apoptosis through the mitochondrial pathway in human breast cancer MDA-MB-231 cells, as evidenced by increases in subG1 cells, phosphatidylserine externalization, loss of MMP, activation of caspase-9 and -3, and cleavage of PARP. Because pretreatment of MDA-MB-231 cells with zVAD-fmk only partly prevented protoapigenone- or apigenin-induced DNA fragmentation, suggesting that the caspase-independent death effectors released from mitochondria, such as apoptosis-inducing factor (AIF), endonuclease G (EndoG), and Omi/HtrA2, may be also involved in the apoptotic induction. On the other hand, prolonged treatment of protoapigenone could also induce necrotic death in MDA-MB-231 cells.

MAPKs have been implicated in mediating apoptosis [27]. Stress-activated JNK and p38 can induce mitochondria-dependent apoptosis in many types of cancer cells [28–30]. Although ERK activation caused by mitogens contributes to cell proliferation and survival, emerging evidence have suggested that stress-activated ERK can exert apoptotic influence when its activation tends to be

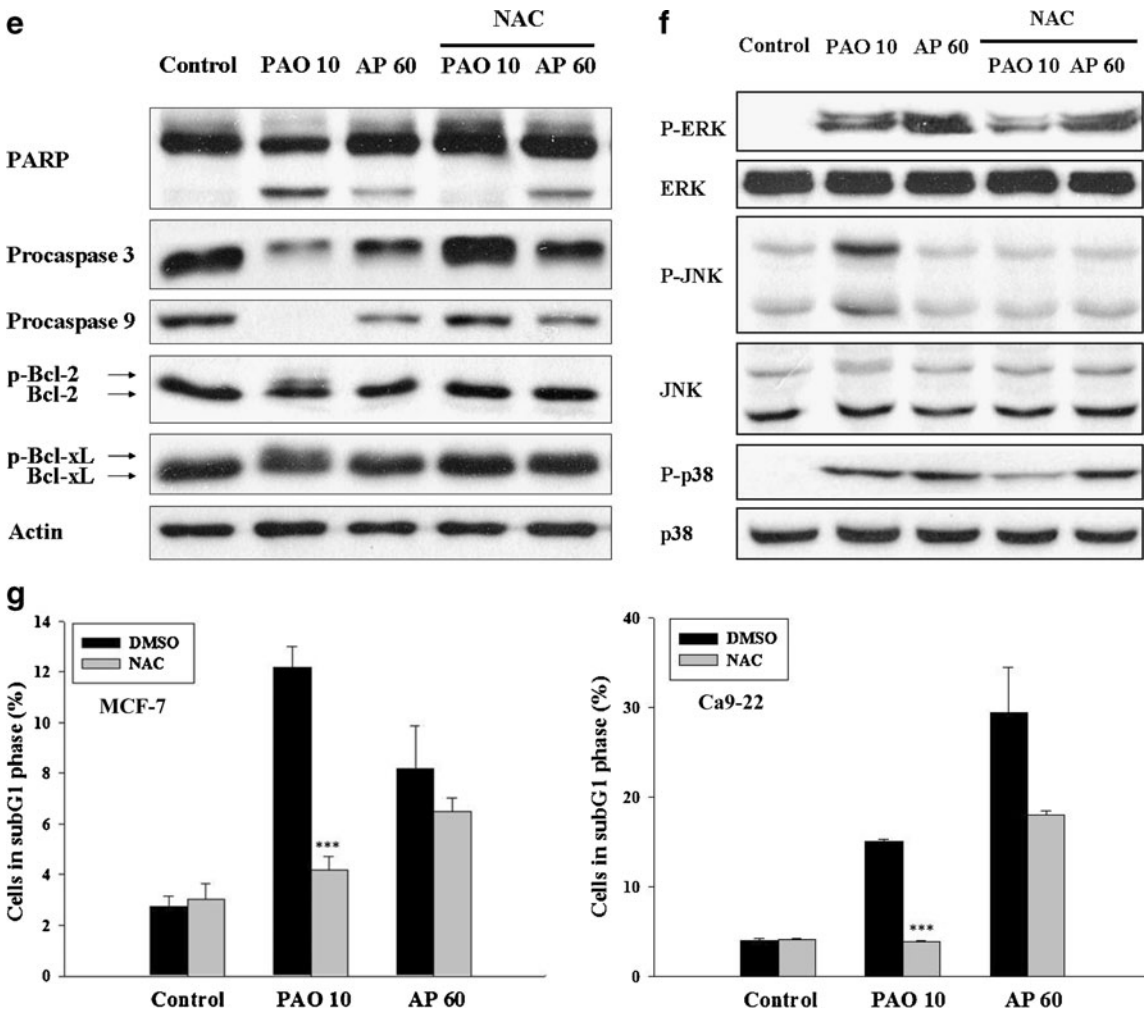

Fig. 6 (continued)

delayed and sustained [20, 27, 31, 32]. In a previous study, protoapigenone was showed to induce activation of JNK and p38 in human prostate cancer cells [11]. We show here that in addition to JNK and p38, protoapigenone also induced persistent activation of ERK. Using selective inhibitors of ERK, JNK, and p38, we have demonstrated that all these MAPKs are involved in protoapigenone-induced apoptosis. Furthermore, the ability of MAPK inhibitors for preventing protoapigenone-induced apoptosis is superior to that of zVAD-fmk, indicating that MAPKs may also mediate caspase-independent apoptotic processes such as mitochondria-released AIF during protoapigenone-induced cell death. Bcl-2 family members are the main site of action for MAPKs in mitochondria. It has been known that MAPKs inhibit the function of antiapoptotic Bcl-2 family members via multiple-site phosphorylation of Bcl-2 or Bcl-xL [33–36]. For example, JNK phosphorylates Bcl-2 at Thr56, Thr69, Ser70, and Ser87 [33, 37], whereas p38 phosphorylates Bcl-2 at only Ser87 and Thr56 [36]. Phosphorylation of Bcl-2 on these residues results in loss of its capacity to heterodimerize with Bax and finally leads to mitochondria-dependent apoptosis [22, 38–41]. In the present work, the hyperphosphorylation of Bcl-2 and Bcl-xL was correlated well with protoapigenone-induced MAPK activation and MTT loss, suggesting that this event might be linked to apoptotic death caused by protoapigenone. In contrast to protoapigenone, though apigenin also elicited activation of MAPKs, it did not induce hyperphosphorylation of Bcl-2 proteins, and MAPK inhibitors failed to prevent mitochondrial dysfunction and apoptosis caused by apigenin. This indicates that MAPK activation is not a prerequisite for apigenin-induced apoptotic death in MDA-MB-231 cells.

The cellular redox state is primary a consequence of the net balance between the levels of ROS and endogenous thiol antioxidants present in cells, which protect cells from oxidative damage. When ROS production exceeds the buffering capacity of thiol antioxidants, cellular oxidative stress increases and leads to sustained activation of MAPKs and apoptosis [42, 43]. Because the mechanism underlying

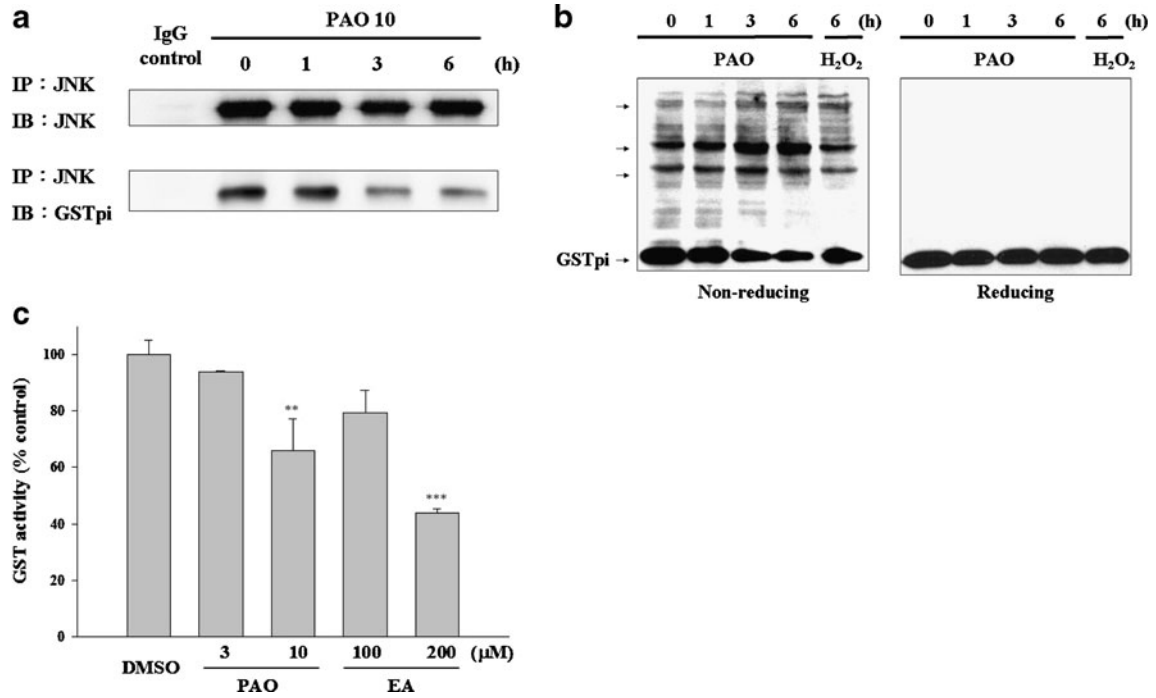

Fig. 7 Effects of protoapigenone on JNK-GSTpi complex association and GSTpi activity. (**a**) Protoapigenone disrupts JNK-GSTpi association. MDA-MB-231 cells were treated with protoapigenone (10 μM) for 1, 3, or 6 h. After treatment, samples were immunoprecipitated with anti-JNK antibody and processed for immunoblot analysis using antibodies to JNK and GSTpi. (**b**) Protoapigenone causes the formation of disulfide-linked GSTpi. Cells were treated with protoapigenone (10 μM) or H_2O_2 (250 μM) for the indicated periods. The disulfide linked-GSTpi were analyzed by non-reducing versus reducing SDS-PAGE. (**c**) Effects of protoapigenone on GSTpi activity. MDA-MB-231 cells were treated with protoapigenone (3 and 10 μM) or ethacrynic acid (100 and 200 μM) for 6 h. The activity of GSTpi was then measured as described in "Materials and Methods". Results are presented as mean±S.E.M. of 3 independent experiments. $^{**}P<0.01$, $^{***}P<0.001$ as compared with control

protoapigenone-induced MAPK activation has not been explored in previous studies [11], we wanted to examine whether protoapigenone activated the MAPK pathway through increasing cellular oxidative stress. In our experiments, protoapigenone induced rapid ROS production and coincidently decreased the glutathione levels in MDA-MB-231 cells, suggesting that protoapigenone disrupted the redox balance and increased cellular oxidative stress. Pretreatment of cancer cells with NAC, which is a thiol antioxidant and a precursor of glutathione, resulted in inhibition of the activation of MAPKs, the phosphorylation of Bcl-2 and Bcl-xL, the loss of MMP, the activation of caspases, the cleavage of PARP, and the apoptosis induced by protoapigenone. These results clearly demonstrated that the change of redox state is an early and crucial event in protoapigenone-induced apoptosis and lies upstream of the signaling molecules including MAPKs. In contrast, although apigenin also markedly induced ROS production and reduced glutathione levels in MDA-MB-231 cells, elimination the oxidative stress by NAC did not reverse apigenin-induced apoptosis, suggesting that redox imbalance is not essential for its cytotoxicity. These results are consistent with a previous study in which protein kinase Cδ, but not ROS and MAPK, played an important role in apigenin-induced apoptosis in leukemia cells [44]. In addition, apigenin has been reported to induce apoptotic death in breast cancer cells through inhibition of the PI3K/Akt pathway [45, 46]. Therefore, apigenin could still exert cytotoxicity by these mechanisms even though ROS production has been prevented by antioxidants. The differences in potency and mechanism of action between apigenin and protoapigenone may be resulted from that protoapigenone, but not apigenin, possesses an α, β-unsaturated ketone moiety in the structure of ring B. We have also previously observed that an analogous of protoapigenone, protoapigenin, which contains a hydroxyl group instead of a ketone in the ring B exhibiting weak antitumor activity [9]. It is known that α, β-unsaturated ketone involved in Michael addition reactions to thiols [47, 48]. Several anticancer agents containing α, β-unsaturated ketone, including doxorubicin, camptothecin, have been shown to exert cytotoxic effects via thiol modification in cancer cells [49–51]. Therefore, protoapigenone may react directly and interfere with cellular thiol-containing molecules that involved in regulating cell survival and death.

GSTpi is one of thiol-containing molecule may affected by protoapigenone. It was known that the Cys47 residue in GSTpi is highly reactive towards unsaturated aldehydes and

ketones and the modification of Cys47 can lead to loss of GSTpi activity [52–54]. Alternatively, formation of inter-subunit disulfide bonds between of cysteine residues of GSTpi upon oxidative stress results in oligomerization of GSTpi and dissociation of GSTpi-JNK complex [25, 55]. In this study, protoapigenone-induced JNK activation was accompanied by the oligomerization of GSTpi and the dissociation of JNK from GSTpi, suggesting that the thiol modification of GSTpi by protoapigenone impeded GSTpi inhibition of JNK and thus facilitate JNK activation. Because protoapigenone decreased GSTpi activity both in vitro and in vivo, it might exert its effect either by inhibiting GSTpi directly or by increasing cellular oxidative stress, which in turn led to inhibition of GSTpi. It is of note that although the in vitro potency of the GSTpi inhibitor ethacrynic acid was greater to that of protoapigenone, its effect on GSTpi in intact cells was much less potent; this may result from the poor cell permeability of ethacrynic acid [56]. Because overexpression of GSTpi in cancer cells is linked to drug resistance, approaches targeting GSTpi have been paid attention to treat resistant malignancies [57, 58]. Therefore, the inhibitory effect of protoapigenone on GSTpi may provide benefit in treating cancer diseases.

In conclusion, we have shown for the first time that the induction of oxidative stress preceding the activation of MAPKs pathways is required to initiate the mitochondria-mediated apoptosis induced by protoapigenone in MDA-MB-231 cells. In particular, inhibition of GSTpi by protoapigenone may be related to JNK activation. Our findings highlight the important potential of protoapigenone to be a promising chemotherapeutic agent for cancer treatment and provide chemical structure information that can be used for the design and development of novel and more effective analogues.

Acknowledgements This work was supported by grants from National Science Council of Taiwan.

References

1. Jemal A, Siegel R, Ward E, Murray T, Xu J, Smigal C, Thun MJ (2006) Cancer statistics, CA. Cancer J Clin 56:106–130
2. Bunz F (2001) Cell death and cancer therapy. Curr Opin Pharmacol 1:337–341
3. Pommier Y, Sordet O, Antony S, Hayward RL, Kohn KW (2004) Apoptosis defects and chemotherapy resistance: molecular interaction maps and networks. Oncogene 23:2934–2949
4. Di Carlo G, Mascolo N, Izzo AA, Capasso F (1999) Flavonoids: old and new aspects of a class of natural therapeutic drugs. Life Sci 65:337–353
5. Middleton E Jr, Kandaswami C, Theoharides TC (2000) The effects of plant flavonoids on mammalian cells: implications for inflammation, heart disease, and cancer. Pharmacol Rev 52:673–751
6. Havsteen BH (2002) The biochemistry and medical significance of the flavonoids. Pharmacol Ther 96:67–202
7. Liu LZ, Fang J, Zhou Q, Hu X, Shi X, Jiang BH (2005) Apigenin inhibits expression of vascular endothelial growth factor and angiogenesis in human lung cancer cells: implication of chemoprevention of lung cancer. Mol Pharmacol 68:635–643
8. Patel D, Shukla S, Gupta S (2007) Apigenin and cancer chemoprevention: progress, potential and promise. Int J Oncol 30:233–245
9. Lin AS, Chang FR, Wu CC, Liaw CC, Wu YC (2005) New cytotoxic flavonoids from Thelypteris torresiana. Planta Med 71:867–870
10. Chang HL, Su JH, Yeh YT, Lee YC, Chen HM, Wu YC, Yuan SS (2008) Protoapigenone, a novel flavonoid, inhibits ovarian cancer cell growth in vitro and in vivo. Cancer Lett 267:85–95
11. Chang HL, Wu YC, Su JH, Yeh YT, Yuan SS (2008) Protoapigenone, a novel flavonoid, induces apoptosis in human prostate cancer cells through activation of p38 mitogen-activated protein kinase and c-Jun NH2-terminal kinase 1/2. J Pharmacol Exp Ther 325:841–849
12. Wu CC, Chan ML, Chen WY, Tsai CY, Chang FR, Wu YC (2005) Pristimerin induces caspase-dependent apoptosis in MDA-MB-231 cells via direct effects on mitochondria. Mol Cancer Ther 4:1277–1285
13. Chen WY, Wu CC, Lan YH, Chang FR, Teng CM, Wu YC (2005) Goniothalamin induces cell cycle-specific apoptosis by modulating the redox status in MDA-MB-231 cells. Eur J Pharmacol 522:20–29
14. Cumming RC, Andon NL, Haynes PA, Park M, Fischer WH, Schubert D (2004) Protein disulfide bond formation in the cytoplasm during oxidative stress. J Biol Chem 279:21749–21758
15. LeBel CP, Ischiropoulos H, Bondy SC (1992) Evaluation of the probe 2′, 7′-dichlorofluorescin as an indicator of reactive oxygen species formation and oxidative stress. Chem Res Toxicol 5:227–231
16. Hou YY, Wu ML, Hwang YC, Chang FR, Wu YC, Wu CC (2009) The natural diterpenoid ovatodiolide induces cell cycle arrest and apoptosis in human oral squamous cell carcinoma Ca9-22 cells. Life Sci 85:26–32
17. Aoshiba K, Yasui S, Nishimura K, Nagai A (1999) Thiol depletion induces apoptosis in cultured lung fibroblasts. Am J Respir Cell Mol Biol 21:54–64
18. Habig WH, Pabst MJ, Jakoby WB (1974) Glutathione S-transferases. The first enzymatic step in mercapturic acid formation. J Biol Chem 249:7130–7139
19. Ono K, Han J (2000) The p38 signal transduction pathway: activation and function. Cell Signal 12:1–13
20. Davis RJ (2000) Signal transduction by the JNK group of MAP kinases. Cell 103:239–252
21. Basu A, Haldar S (2003) Identification of a novel Bcl-xL phosphorylation site regulating the sensitivity of taxol- or 2-methoxyestradiol-induced apoptosis. FEBS Lett 538:41–47
22. Brichese L, Cazettes G, Valette A (2004) JNK is associated with Bcl-2 and PP1 in mitochondria: paclitaxel induces its activation and its association with the phosphorylated form of Bcl-2. Cell Cycle 3:1312–1319
23. Fleury C, Mignotte B, Vayssière JL (2002) Mitochondrial reactive oxygen species in cell death signaling. Biochimie 84:131–141
24. Carvalho H, Evelson P, Sigaud S, González-Flecha B (2004) Mitogen-activated protein kinases modulate H(2)O(2)-induced apoptosis in primary rat alveolar epithelial cells. J Cell Biochem 92:502–513
25. Adler V, Yin Z, Fuchs SY, Benezra M, Rosario L, Tew KD, Pincus MR, Sardana M, Henderson CJ, Wolf CR, Davis RJ, Ronai Z (1999) Regulation of JNK signaling by GSTp. EMBO J 18:1321–1334
26. Matsuzawa A, Ichijo H (2005) Stress-responsive protein kinases in redox-regulated apoptosis signaling. Antioxid Redox Signal 7:472–481

27. Wada T, Penninger JM (2004) Mitogen-activated protein kinases in apoptosis regulation. Oncogene 23:2838–2849
28. Martindale JL, Holbrook NJ (2002) Cellular response to oxidative stress: signaling for suicide and survival. J Cell Physiol 192:1–15
29. Selimovic D, Hassan M, Haikel Y, Hengge UR (2008) Taxol-induced mitochondrial stress in melanoma cells is mediated by activation of c-Jun N-terminal kinase (JNK) and p38 pathways via uncoupling protein 2. Cell Signal 20:311–322
30. Kang YH, Lee SJ (2008) Role of p38 MAPK and JNK in enhanced cervical cancer cell killing by the combination of arsenic trioxide and ionizing radiation. Oncol Rep 20:637–643
31. Sakon S, Xue X, Takekawa M, Sasazuki T, Okazaki T, Kojima Y, Piao JH, Yagita H, Okumura K, Doi T, Nakano H (2003) NF-kappaB inhibits TNF-induced accumulation of ROS that mediate prolonged MAPK activation and necrotic cell death. EMBO J 22:3898–3909
32. Nakano H, Nakajima A, Sakon-Komazawa S, Piao JH, Xue X, Okumura K (2006) Reactive oxygen species mediate crosstalk between NF-kappaB and JNK. Cell Death Differ 13:730–737
33. Yamamoto K, Ichijo H, Korsmeyer SJ (1999) BCL-2 is phosphorylated and inactivated by an ASK1/Jun N-terminal protein kinase pathway normally activated at G(2)/M. Mol Cell Biol 19:8469–8478
34. Fan M, Goodwin M, Vu T, Brantley-Finley C, Gaarde WA, Chambers TC (2000) Vinblastine-induced phosphorylation of Bcl-2 and Bcl-XL is mediated by JNK and occurs in parallel with inactivation of the Raf-1/MEK/ERK cascade. J Biol Chem 275:29980–29985
35. Deng X, Xiao L, Lang W, Gao F, Ruvolo P, May WS Jr (2001) Novel role for JNK as a stress-activated Bcl2 kinase. J Biol Chem 276:23681–23688
36. De Chiara G, Marcocci ME, Torcia M, Lucibello M, Rosini P, Bonini P, Higashimoto Y, Damonte G, Armirotti A, Amodei S, Palamara AT, Russo T, Garaci E, Cozzolino F (2006) Bcl-2 Phosphorylation by p38 MAPK: identification of target sites and biologic consequences. J Biol Chem 281:21353–21361
37. Maundrell K, Antonsson B, Magnenat E, Camps M, Muda M, Chabert C, Gillieron C, Boschert U, Vial-Knecht E, Martinou JC, Arkinstall S (1997) Bcl-2 undergoes phosphorylation by c-Jun N-terminal kinase/stress-activated protein kinases in the presence of the constitutively active GTP-binding protein Rac1. J Biol Chem 272:25238–25242
38. Srivastava RK, Mi QS, Hardwick JM, Longo DL (1999) Deletion of the loop region of Bcl-2 completely blocks paclitaxel-induced apoptosis. Proc Natl Acad Sci USA 96:3775–3780
39. Ruvolo PP, Deng X, May WS (2001) Phosphorylation of Bcl2 and regulation of apoptosis. Leukemia 15:515–522
40. Fulda S, Debatin KM (2006) Extrinsic versus intrinsic apoptosis pathways in anticancer chemotherapy. Oncogene 25:4798–4811
41. Poommipanit PB, Chen B, Oltvai ZN (1999) Interleukin-3 induces the phosphorylation of a distinct fraction of bcl-2. J Biol Chem 274:1033–1039
42. Simon HU, Haj-Yehia A, Levi-Schaffer F (2000) Role of reactive oxygen species (ROS) in apoptosis induction. Apoptosis 5:415–418
43. Boonstra J, Post JA (2004) Molecular events associated with reactive oxygen species and cell cycle progression in mammalian cells. Gene 337:1–13
44. Vargo MA, Voss OH, Poustka F, Cardounel AJ, Grotewold E, Doseff AI (2006) Apigenin-induced-apoptosis is mediated by the activation of PKCdelta and caspases in leukemia cells. Biochem Pharmacol 72:681–692
45. Way TD, Kao MC, Lin JK (2004) Apigenin induces apoptosis through proteasomal degradation of HER2/neu in HER2/neu-overexpressing breast cancer cells via the phosphatidylinositol 3-kinase/Akt-dependent pathway. J Biol Chem 279:4479–4489
46. Lee WJ, Chen WK, Wang CJ, Lin WL, Tseng TH (2008) Apigenin inhibits HGF-promoted invasive growth and metastasis involving blocking PI3K/Akt pathway and beta 4 integrin function in MDA-MB-231 breast cancer cells. Toxicol Appl Pharmacol 226:178–191
47. Olmos G, Conde I, Arenas I, Del Peso L, Castellanos C, Landazuri MO, Lucio-Cazana J (2007) Accumulation of hypoxia-inducible factor-1alpha through a novel electrophilic, thiol antioxidant-sensitive mechanism. Cell Signal 19:2098–2105
48. Böhme A, Thaens D, Paschke A, Schüürmann G (2009) Kinetic glutathione chemoassay to quantify thiol reactivity of organic electrophiles application to alpha,beta-unsaturated ketones, acrylates, and propiolates. Chem Res Toxicol 22:742–750
49. Radin NS (2003) Designing anticancer drugs via the achilles heel: ceramide, allylic ketones, and mitochondria. Bioorg Med Chem 11:2123–2142
50. Bradshaw TD, Matthews CS, Cookson J, Chew EH, Shah M, Bailey K, Monks A, Harris E, Westwell AD, Wells G, Laughton CA, Stevens MF (2005) Elucidation of thioredoxin as a molecular target for antitumor quinols. Cancer Res 65:3911–3919
51. Chen WY, Chang FR, Huang ZY, Chen JH, Wu YC, Wu CC (2008) Tubocapsenolide A, a novel withanolide, inhibits proliferation and induces apoptosis in MDA-MB-231 cells by thiol oxidation of heat shock proteins. J Biol Chem 283:17184–17193
52. van Iersel ML, Ploemen JP, Lo Bello M, Federici G, van Bladeren PJ (1997) Interactions of alpha, beta-unsaturated aldehydes and ketones with human glutathione S-transferase P1-1. Chem Biol Interact 108:67–78
53. Bogaards JJ, Venekamp JC, van Bladeren PJ (1997) Stereoselective conjugation of prostaglandin A2 and prostaglandin J2 with glutathione, catalyzed by the human glutathione S-transferases A1-1, A2-2, M1a-1a, and P1-1. Chem Res Toxicol 10:310–317
54. van Zanden JJ, Ben Hamman O, van Iersel ML, Boeren S, Cnubben NH, Lo Bello M, Vervoort J, van Bladeren PJ, Rietjens IM (2003) Inhibition of human glutathione S-transferase P1-1 by the flavonoid quercetin. Chem Biol Interact 145:139–148
55. Shen H, Tsuchida S, Tamai K, Sato K (1993) Identification of cysteine residues involved in disulfide formation in the inactivation of glutathione transferase P-form by hydrogen peroxide. Arch Biochem Biophys 300:137–141
56. Wang R, Li C, Song D, Zhao G, Zhao L, Jing Y (2007) Ethacrynic acid butyl-ester induces apoptosis in leukemia cells through a hydrogen peroxide mediated pathway independent of glutathione S-transferase P1-1 inhibition. Cancer Res 67: 7856–7864
57. Tew KD, Ronai Z (1999) GST function in drug and stress response. Drug Resist Updat 2:143–147
58. Townsend DM, Tew KD (2003) The role of glutathione-S-transferase in anti-cancer drug resistance. Oncogene 22: 7369–7375